A&A manuscript no.
(will be inserted by hand later)

Your thesaurus codes are:
03check this (08.06.2; 09.08.1; 11.09.2; 11.16.2; 11.19.3; 13.18.1)

ASTRONOMY AND ASTROPHYSICS

Star Formation Histories in H II Galaxies

II: Integrating Optical and Radio Results

H.J. Deeg[1], E. Brinks[2], and N. Duric[3]

[1] Instituto de Astrofisica de Canarias,c/ Via Lactea s/n,38200 La Laguna, Canary Islands, Spain, (email: hdeeg@iac.es)
[2] Universidad de Guanajuato, Guanajuato, Gto. 36000, Mexico
[3] Institute for Astrophysics, Dept. of Physics and Astronomy, University of New Mexico, Albuquerque, NM 87131, USA

unpublished manuscript with copyright by the authors. Version of 18 November 1997

Abstract. For a sample of eight H II galaxies with strong radio continuum emission, star formation rate (SFR) indicators and star formation age indicators are derived and compared, based on radio and optical measurements introduced in previous papers. The best SFR indicator for the most recent (0-3 Myrs) star formation is the thermal radio emission, which can be calibrated reliably using a combination of radio continuum spectra and Ha photometry. Other SFR indicators giving recent SFRs are the FIR emission, which gives SFRs over the last 10 Myrs and the nonthermal radio emission, which gives the SFR as it was 3-10 Myrs ago. The long term (1 Gyr) SFRs based on B band photometry are relatively much lower. This indicates that these H II galaxies are indeed having recent and enhanced star formation, probably triggered by some interaction event, for which there are indications in all sample galaxies. This hypothesis is supported by indiactors of the *age* of the most recent star forming. For some galaxies with characteristic knees in the radio spectra, synchrotron aging indicates major changes in the SFR a few Myrs ago. Similar star ages of star forming events are derived, based on the ratio of the FIR-to-thermal radio emission. Ages derived from optical U-B and B-R colors indicate much higher ages for the star formation, though. The inability of stellar colors to indicate very recent changes in the SFR at time scales of $\lesssim 10^7$ Myrs, and the absence of detailed U band photometry are the likely causes for this discrepancy. Based on the star formation rates and the age indicators, the galaxies were sorted into a sequence of the age of their starbursts. A correlation between the fraction of thermal emission and size, as well as total luminosity of the galaxies has been found. By comparing different star formation estimators based on a variety of radiative processes and across three regions of the electromagnetic spectrum, it is now possible to paint a coherent picture of a region of active star formation in which SN explosions take place, and to understand and account for the thermal and nonthermal radiation which is generated.

Send offprint requests to: H.J. Deeg

Key words: –

1. Introduction

In this paper we bring together radio and optical observations of a sample of radio-bright H II galaxies and combine our results with analytical models in order to try to understand their unusual radio spectra. The H II regions in H II galaxies have sizes of a few 100 pc and are several orders of magnitude larger than well studied star forming regions in the Milky Way, like the Orion complex. They may contain on the order of 10^4 very young and hot O stars. They resemble major star formation regions such as 30 Doradus in the LMC or NGC 604 in M33 (Wilson and Scoville, 1992). In H II galaxies, the radiation from the H II regions is often dominating. The extraction of information about the history and physical properties of starforming regions in H II galaxies is therefore simpler than in normal galaxies, where background radiation from older stellar populations is often dominating. This makes H II galaxies ideally suited to study the radiation from star-forming regions by measuring their global emission. The goal of this work is to reconstruct the recent star formation histories for a small sample of H II galaxies by obtaining an integral view of the footprints of a star forming event at a range of observable wavelengths including radio, optical and the far infrared (FIR).

Radiation at radio wavelengths is a primary indicator for star formation. Observations of the radio spectra of a small sample of H II galaxies at low frequencies (325 MHz) in Deeg et al. (1993, hereafter DBDKS) showed that there are breaks in the radio spectra of some of these galaxies. The first central question, already addressed by DBDKS, and introduced again in this paper is:

1) What is the origin of the radio emission and what determines the shape of the radio spectra of H II *galaxies?*

The data which we use in this paper are the results published by DBDKS, and more recent data by Deeg et

al. (1997, hereafter Paper I). The breaks in the spectra can not be explained via a simple superposition of synchrotron (nonthermal) and thermal power law spectra (Klein, Weiland and Brinks, 1991). Other galaxies with similar breaks in their radio spectra have been investigated by Israel and de Bruyn (1988); Israel and Mahoney (1990); Pohl and Schlickeiser (1990); Pohl, Schlickeiser and Hummel (1991) and Hummel (1991). All of these authors have in common that they attempted to explain the observed spectra by considering one mechanism only in order to expain the radio spectra. A more comprehensive approach has been taken by DBDKS; a variety of mechanisms is introduced and then judged according to their capability to explain the observed spectra. There are two major mechanisms which were investigated in detail. The first one, synchrotron aging, explains the spectral breaks by variations in the injection rate of relativistic electrons into the interstellar medium. It is developed using several different scenarios for the history of the relativistic or cosmic ray electron (CRE) injection. A full exploration of this method could result in a new and independent indicator for changes in the history of the CRE injection rate. As CRE are generated in supernova remnants over a time of 10^4 to 10^5 years after a type II supernova explosion, the CRE injection rate can serve as an indicator for the recent supernova rate. The other mechanism discussed by DBDKS is a combination of free-free absorption of low frequency radio waves in the ionized ISM and thermal radio emission, which dominates at high frequencies. Modelling these mechanisms allows one to derive a number of physical parameters which reveal information about the conditions in the star forming region (i.e. gas densities, magnetic field strength, star burst ages and temporal variations in the generation of relativistic electrons). Strong starforming events, lasting for a few Myrs, and the resulting temporal variations in the number of relativistic electrons injected into the ISM from type II supernovae were judged to be the most likely cause for the observed spectral shapes. Consequently, the interpretation of the shapes of the radio spectra allows one to estimate the time scale over which the star formation occured. Some of the methods used by DBDKS and others to interpret radio spectra have been applied to a few cases only and the results have not been compared to data from optical and FIR observations in a self-consistent way. This leads to the second topic addressed in this paper:

2) How do the radio spectra relate to indicators of star formation rates (SFRs) and star formation histories which are based on a variety of other techniques and using data from other wavelength domains?

In Paper I, we performed CCD photometry and determined integrated and surface magnitudes of the galaxies in B,R and I filters and produced surface color maps of the sample. Hα fluxes derived from narrow band imaging were combined with best fits from the radio data to derive the galaxies' thermal flux and the location of the star forming regions. As we discussed in Paper I, the broadband surface colors are correlated with the location of starforming regions in some galaxies, whereas in others, extinction obscures the underlying starforming activity.

A variety of indicators for the star formation histories as well as star formation rates can be derived from the combination of the radio data with the results from the optical observations presented in Paper I, as well as by their combination with FIR and UV observations from the literature. These data are used as independent indicators of the star forming activity. Fundamental work on estimates of star formation rates, and their changes throughout time, mostly based on optical observations, has been presented by Kennicutt (1983) and Gallagher, Hunter and Tutukov (1984). They developed a set of simple formulae to obtain star formation rates from optical luminosities. Another approach, which was taken for the optical as well as the radio data, is a comparison with results from analytical models (Belfort, Mochkovitch and Dennefeld 1987; Scoville et al. 1991) or computer models which simulate the properties of galaxies throughout a starburst (e.g. Mas-Hesse 1992; Mas-Hesse and Kunth 1991; Charlot and Bruzual 1991; Krüger et al. 1991). These approaches have been used to obtain a series of estimates about the recent star formation histories of these galaxies, including a range of cross-checks between these estimates from the various wavelength domains.

2. Deriving the star formation history from optical and radio results

In this section, a synthesis of the results from the interpretation of the radio data by DBDKS and of the optical data introduced in Paper I is attempted by comparing star formation rates (SFRs) and ages, derived from the various data. Before discussing any derived results, an overview is given in Table 1 of the luminosities and other quantities relevant for the derivation of SFRs and star formation histories. All luminosities were derived using the distances listed in Table 1 of DBDKS, which are based on H_o = 75 km $s_{-1}Mpc_{-1}$(Haro 1, not included in DBDKS, is assumed to be at a distance of 50.2 Mpc). The rows of Table 1 show the following quantities:

- D_{25} : Diameter D_{25} from the RC3 (de Vaucouleurs et al., 1991), in kpc
- L_B : the B-band luminosity, based on the absolute corrected B-band magnitude $B°_T$ from the RC3 (Table 3b, Paper I). It is expressed in units of bolometric solar luminosities (see discussion in section 2.3). L_{FIR} : The FIR Luminosity, from Wunderlich (1987), see also Table 1 in DBDKS
- $f_{th,1.49}$: The fraction of thermal radio emission of the total radio emission at 1.49 GHz, from $f_{th,adopt,1.49GHz}$ in Table 7 of Paper I.

Table 1. Luminosities and other quantities needed for the derivation of SFRs

	Haro 15	II Zw 40	Haro 1	II Zw 70	Mkn 297	Mkn 314	Mkn 527	III Zw 102
Distance(Mpc)	86	10.1	50	17.1	64	31	50	25
D_{25} (kpc)	21	0.97	13.3	3.7	17.4	8.3	21	11.5
$L_B(10^9 L\odot)$	6.0	0.13	4.8	0.14	3.8	0.65	1.6	1.1
$L_{FIR}(10^9 L\odot)$	22.0	1.49	47.7	0.51	62.2	2.57	25.2	13.8
$f_{th1.49}$	0.15±.09	0.75±.1	0.26±.04	0.70±.1	0.07±. 04	0.50±.1	0.60±.06	0.12±.06
$L_{tot1.49}(10^{27} ergHz^{-1}s^{-1})$	203±44	3.7±0.2	170±9	1.60±.35	510±34	7.4±0.7	20.0±1.0	37±2
$L_{th1.49}(10^{27} ergHz^{-1}s^{-1})$	31±20	2.8±0.4	44±7	1.1±0.3	33±20	3.7±0.9	11.7±1.3	4.5±2.3
N_{Ostars}	1.4E5	1.4E4	2.0E5	5.1E3	1.5E5	1.7E4	5.4E4	2.1E4
$\alpha(6,20)$	-0.47±.22	-0.27±.12	-0.45±.09	-0.35±.45	-0.75±.07	-0.48±.12	-0.34±.10	-0.56±.08

Table 2. Star formation rates for stars with masses $M > 5M\odot$

	age(Myr)	Haro 15	II Zw 40	Haro 1	II Zw 70	Mkn 297	Mkn 314	Mkn 527	III Zw 102
SFR_{th}	0-3	5.8±3.9	0.52±.08	8.3±1.3	0.21±.06	6.3±3.8	0.69±.16	2.2±.2	0.86±.43
SFR_{fir}	0-10	4.9±.5	0.33±.3	10.7±.9	0.11±.01	14±1	0.58±.05	5.6±.7	3.1±.3
SFR_{nth}	3-10	4.1±1.1	.023±.01	3.4±.3	.015±.01	12.4 ±1.1	.087±.02	0.21±.04	0.79±.08
SFR_B	0-1000	0.17	0.0038	0.14	0.0040	0.11	0.019	0.047	0.032

Notes: SFR_{th}: based on thermal radio emission. SFR_{fir}: based on FIR emission. SFR_{nth}: based on nonthermal radio emission. SFR_B: based on optical B magnitude.

- $L_{tot,1.49}$: The total radio luminosity at 1.49 GHz, from $S_{totalRad,1.49GHz}$ in Table 7 of Paper I.
- $L_{th,1.49}$: The thermal luminosity at 1.49 GHz, derived from $L_{tot,1.49}$ and $f_{th,1.49}$.
- N_{Ostar} : The number of OV stars with spectral class that correspond to $L_{th,1.49}$. An IMF with a spectral index of -2.5 was assumed.
- $\alpha(6,20)$: The radio spectral index derived from 6 and 20 cm flux densities, with flux values taken from DBDKS and paper I.

Table 2 gives an overview of the derived SFRs, derived from the indicators which are discussed in the following sections. The column labelled 'age' in Table 2 gives the approximate time span in the past, over which this SFR is averaged. Errors for the SFRs are based only on the errors of the corresponding measurement, but not on any uncertainties (which are not quoted in the literature) in the factors in the formulae which convert the measurements into SFRs. The optical and the radio data are direct or indirect indicators of the emissions of *all* stars in a star forming region. These stars may cover a wide range of masses and may be at several stages of development, including SNe. Furthermore, indirect emissions such as radio emission and at least part of the FIR depend on the physical condition of the ISM in the star forming region. Therefore, the various SFR indicators (from Table 2) do not give the SFR for *all* stars directly, but they are generally indicative of stars in a certain mass range or at a certain development stage only. For example, the SFR derived from the non-thermal emission depends on the rate of type II supernova explosions per year - and only stars with masses M $\gtrsim$ 6 to 8 $M\odot$[1] are thought to undergo such an event.

To convert a SFR derived for one mass range to the total star formation rate, i.e. the SFR indicating the mass of all stars born, the initial mass function (IMF) needs to be known, which describes the number of stars born in a certain mass-interval. The IMFs are usually expressed as power laws of the form:

$$\Phi(M) = dN/dM \sim M^{-\alpha} \quad (1)$$

where we dN/dM is the numbers of stars formed per mass-interval. If dN is taken to be in units of the number of stars (of mass M) formed per year, the SFR can then be derived by:

$$SFR = \int M\Phi(M)dM \quad (2)$$

Besides the uncertainty of α in the IMF, the derivation of the SFR also requires an assumption about the range of masses, for which the IMF is valid. Whereas the upper limit, which is usually taken as 100-120 $M\odot$, is not very critical, at the lower mass limit, $\Phi(M)$ goes to infinity for a > 1. Often, the lower mass limit is set to 0.1 $M\odot$ although the lower mass limit for the ignition of a fusion reaction in a star is thought to be 0.08 $M\odot$. The simplest IMF in common use is Salpeter's (1955) IMF with $\alpha = 2.35$. A frequent modification is the use of different values of a for low-mass and high mass stars, e.g. Kennicutt (1983) adopts a modified 'Miller-Scalo (1979) IMF[2] with:

$$\Phi(M) \propto M^{-1.4} (0.1 \leq M \leq 1M\odot) \quad (3)$$
$$\Phi(M) \propto M^{-2.5} (1 \leq M \leq 100M\odot)$$

Note that the IMFs quoted were derived from observations of the solar neighborhood. Modifications for an environment in which active, massive star formation takes

[1] The mass range from 6 to 8 $M\odot$ is most commonly cited in the literature as the lower limit for SNs.

[2] The original IMF derived by Miller and Scalo (1979) uses $\Phi(M) \propto M^{-3.3}$ for $10 \leq M \leq 100M\odot$

place are very uncertain. So far, model calculations for star forming dwarf galaxies use IMFs very close to eq. (3) (e.g. Krüger et al., 1991) or vary the index of the IMF's power law over a wide range (Mas-Hesse, 1992, hereafter M92). There are strong indications that in a starbursting environment, higher mass stars are formed preferentially, with the upper mass limit of the stars formed decreasing throughout the star formation event (Wright et al., 1988).

In the star-formation models, commonly two ideal star-formation scenarios are assumed: The instantenous burst (IB) model assumes that all stars in a particluar burst-event formed at the same time. Since the SFR has a delta-shape in such an event, it cannot be assigned numerical values and only the overall number of stars formed in the event can be expressed. The other extreme is the "continous star formation rate (CSFR)" model, were a zero SFR is assumed before the begin of the starformation event, which then proceeded with a continous, unchanging rate until the present. In reality, SFR's can be assumed to vary sigificantly over time-scales of several million years, and realistic star-formation events (and the consequent emissions at various wavelengths) could be modeled by a convolutiuon of IB models with functions giving the SFR over time.

In the following sections, we give SF*rates* with the following definition: The SFR's give the *average* rate of the SF over the convolution time-scale to which the particluar emission (for example Hα) is sensitive. For example, if Hα emission is excited by massive stars younger then 5 Myrs, the convolution time scale is from 5 Mrs in the past to the present, and the SFR based on H*alpha* emission gives the average SFR over the last 5 Myrs. SFRs quoted with this definiton are roughly equivalent to SFR's derived from CSFR models, where the SF event began before the convolution time-scale.

2.1. Current star formation derived from thermal and FIR emission

The thermal radio emission, the Hα emission, and to a lesser degree the FIR emission are proportional to the number of ionizing Lyman continuum photons emitted by the young hot stars with $M \gtrsim 5M\odot$ inside the H II region. Based on Kennicutt's (1983) equation for SFRs based on Hα luminosities, Condon (1992) gives the following SFRs derived on the basis of thermal radio-fluxes:

$$\frac{SFR_{th}(M>5M\odot)}{M\odot\ yr^{-1}} = 0.1{\cdot}10^{27}\left(\frac{\nu}{GHz}\right)^{0.1}\frac{L_{th1.49}}{erg\ Hz^{-1}s^{-1}} \quad (4)$$

For SFRs based on the FIR luminosity, the relation given by Sauvage and Thuan (1992) can be converted to $M > 5M\odot$ using the Salpeter IMF, leading to:

$$\frac{SFR_{FIR}(M>5M\odot)}{M\odot yr^{-1}} = 0.22\cdot 10^{-9}\frac{L_{FIR}}{L\odot} \quad (5)$$

The SFRs derived from relations (4) and (5) are listed in Table 2. The SFRs derived from FIR fluxes agree relatively well with those from the thermal radio fluxes within about a factor of two, with the exception of III Zw 102, which is dust rich and may have an elevated FIR emission. Besides uncertainties in the measurements and in the conversion formulae, the ratio between the thermal and FIR luminosities is expected to vary with time throughout a starburst, which consequently leads to varying ratios of SFR_{th} and SFR_{FIR}. The thermal radio luminosity is proportional to the number of emitted Lyc photons inside the H II regions, N_{Lyc}, by (from eq. 12 in Lequeux, 1980):

$$\left(\frac{L_{th}}{erg\ s^{-1}}\right) = 1.598\cdot 10^{-26} f \left(\frac{N_{Lyc}}{photons\ s^{-1}}\right) \times \left(\frac{\nu}{GHz}\right)^{-0.1}\left(\frac{T_e}{10^4 K}\right)^{0.45} \quad (6)$$

where $f \approx 0.7$ (Mas-Hesse and Kunth, 1991, -hereafter MK91-, and Belfort, Mochkovitch and Dennefeld, 1987) is the fraction of the number of Lyc photons absorbed by the gas; (1-f) is the fraction of the Lyc photons absorbed by dust. The Lyc photons are emitted by hot stars of spectral classes O to about B5 with stellar lifetimes of 1 Myr to about 70 Myrs. For tables indicating N_{Lyc} versus stellar spectral class, see MK91.

FIR emission is blackbody radiation emitted by dust of temperatures of a few times 10 K. Models of the FIR emission therefore have to account for the energy sources which heat the dust. Major attributable sources (MK91) are:

- a fraction of (1-f) of the Lyc photons which is absorbed by the dust and heats it.
- a fraction of the radiation longward from the Lyc limit of 912 Å(which is emitted by stars of all masses) is absorbed by the dust. This fraction can be estimated from the internal extinction E(B-V) within the H II regions, which can be obtained observationally from the Hα to Hβ line intensity ratio (Balmer decrement), under the assumption of some extinction law.
- Lyαa photons which are trapped with high efficiency inside the HII region and which are eventually absorbed by a dust grain.
- FIR emission from non-starforming cirrus-like regions. Sauvage and Thuan (1992) argue that this can contribute substantially to the FIR emission, depending on the Hubble type of a galaxy. For Sa galaxies (Mkn 527 and possibly III Zw 102 are classified as such) they quote a cirrus contribution of 86±7 %.

Since N_{Lyc} and thus the thermal luminosity L_{th} (as well as the Hα and Hb line emission) is strongly dependent on the number of very short lived O stars inside the H II region, the thermal radio emission gives a measure of the SFR averaged over approximately the last 3 Myrs (see Fig.3 in MK91). In fact, L_{th} is the star formation

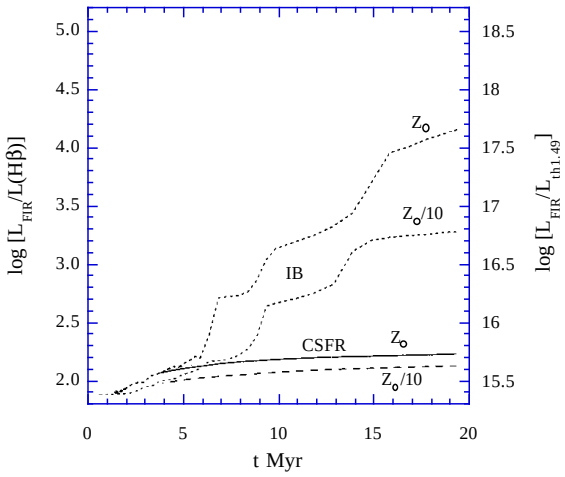

Fig. 1. Evolution of the ratio L_{FIR} to L(Hβ) with time from Mas-Hesse and Kunth (1991) (adapted from their Figs. 14 and 15, using models with E(B-V)=0.01). 'IB' denotes a model of an instantaneous starburst (IB) at t=0 and is calculated for metallicities of Z$\odot$ and Z$\odot$/10. 'CSFR' is a model with a starburst with constant star formation rate since t=0, for Z$\odot$ (solid line) and Z$\odot$/10 (dashed line). A scale indicating log[$L_{FIR}/L_{th1.49}$] was added to the axis on the right side.

parameter reacting the quickest to changes in the SFR. The FIR emission is only partially dependent on N_{Lyc}, and follows the near-UV emission at 3000Åmore closely (compare Fig.3, 6b and Fig. 12 in MK91). For star forming regions with high internal extinction, the FIR emission becomes a good indicator of the sum of the luminosity of all stars with $M \gtrsim 2M\odot$ in the H II region. The FIR emission decreases in about 3-4 Myrs after an instantaneous (delta-shaped) starburst, but not as fast as the thermal emission and will then remain relatively constant. A reasonable estimate is that L_{FIR} indicates the average SFR over the last 10 Myrs.

As one example for the variation between L_{th} and L_{FIR}, Fig. 1 shows the results from evolutionary population synthesis models in starbursts by MK91. These authors calculated the ratio of luminosities [L_{FIR}/L(Hβ)] for two star formation scenarios, assuming negligible internal extinction. One scenario assumes an instantaneous starburst (IB) at t=0, the other one assumes a starburst with constant star formation rate (CSFR) since t=0. The ratio [$L_{FIR}/L_{th1.49}$] is expected to behave identical to the ratio of L_{FIR}/L(Hβ) on which Fig. 1 is based on, since the luminosities L_{th}, and the *intrinsic* luminosities of L(Hα), and L(Hβ) are all proportional to N_{Lyc}. Using the standard ratio of the Balmer line intensities: Hβ / Hα = 1 / 2.86 (see in Paper I: Section 2.5 and eq. 3) it follows that: log[$L_{FIR}/L_{th1.49}$] = 13.5 + log[L_{FIR}/L(Hβ)]. A scale of log[$L_{FIR}/L_{th1.49}$] was added to the right side of Fig. 1. For ease of comparison, values of log[$L_{FIR}/L_{th1.49}$] for the eight sample galaxies are given in Table 3. The table gives mean ages $t_{IB,mean}$ based the log($L_{FIR}/L_{th1.49}$) values in Fig. 1, using the instantaneous star burst scenario (IB) with a metallicity of Z$\odot$ /10 , to account for the low heavy element abundance in H II galaxies. Based on the errors in log($L_{FIR}/L_{th1.49}$), a range of plausible ages for the instantaneous burst scenario, $t_{IB,range}$, is also indicated. For values of log($L_{FIR}/L_{th1.49}$) $\leq$ 15.4, an age of t_{IB} = 0 was assigned. It should be noted, that for realistic SF scenarios that are in-between the extremes of the IB and the CSFR models (in which the $L_{FIR}/L_{th1.49}$ ratios can be expected to lie in between the extremes given by the IB and CSFR model), only the minima of the age ranges ($T_{IB,range}$ are valid, whereas no constraint can be derived to the maximum ages of a Star-burst.

For most galaxies, the $L_{FIR}/L_{th1.49}$ values are low and are consistent with both the constant star formation rate and the instantaneous burst scenarios, only two galaxies (Mkn 527, III Zw 102) are incompatible with a CSFR model. In the age estimates based on the FIR luminosity, the possible contribution of cirrus, or from the underlying galaxy, to the FIR fluxes was not taken into account, as it is impossible to assign Hubble types to most of our objects. In any case, a lower intrinsic FIR luminosity would indicate that the SF event is younger than assumed from Fig.1.

2.2. Star formation rates from nonthermal emission

Nonthermal emission is the direct result of cosmic ray (relativistic) electrons (CRE) gyrating in a magnetic field. These electrons may be initially accelerated in a supernova remnant, although other acceleration mechanisms can't be excluded. The nonthermal luminosity of a galaxy depends on the number of supernova events that occur during the lifetime of the CRE. As even the most massive stars need to be about 3 Myrs old before becoming a SN, the SFR reported by nonthermal radio emission is that of at least 3 Myrs in the past, and includes contributions from older SN events up to the typical lifetime of the CREs. A reasonable estimate may be that the nonthermal radio emission gives the average of the SFR between 3 to 10 Myrs in the past. For models describing the development of the nonthermal luminosity after a starburst, see MK91. Condon (1992) provides the following two equations to derive the SN rate from the non-thermal luminosity, assuming continous starformation:

$$\frac{\nu_{SN}}{yr^{-1}} \approx \frac{1}{13}\left(\frac{\nu}{GHz}\right)^{\alpha_{nth}} \frac{L_{nth}}{10^{29}\ erg\ s^{-1}\ Hz^{-1}} \qquad (7)$$

which connects the SN rate to the nonthermal emission (Condon and Yin, 1990); to obtain the SFR from the SN rate then:

$$\frac{SFR_{nth}(M > 5M\odot)}{M\odot\ yr^{-1}} = 24.4 \cdot \frac{\nu_{SN}}{yr^{-1}} \qquad (8)$$

Condon emphasizes in the summary of his review the need for direct estimates of the SN rate to pin down the

Table 3. FIR to thermal emission ratios

Name	Haro 15	II Zw 40	Haro 1	II Zw 70	Mkn 297	Mkn 314	Mkn 527	III Zw 102
$\log[L_{FIR}/L_{th1.49}]$	15.44±.36	15.34±.18	15.62±.18	15.24±.23	15.85±.34	15.43±.22	15.91±.15	16.07±.31
$T_{IB,mean}$(Myr)	2.5	0	6	0	9	3	9	9
$T_{IB,range}$(Myr)	0-9	0-5	0(3)-9	0-4	0(4)-12	0-7	0(8)-10	0(8)-14

relation between nonthermal luminosity and the SFR. In other words, the proportionality factor between the supernova rate and the nonthermal luminosity in eq. (7) is very uncertain. For example, M92 uses a variation of a factor 's' within a range of 1 to 120 for the strength of the nonthermal emission. This factor is a product of the average absolute power of SNe, the efficiency of the conversion of that power into CRE in the SN resp. SNR, and the efficiency of the conversion of the CRE energy into synchrotron radiation.

At this point we would like to point out a remarkable correlation among the sample galaxies between the thermal fraction, f_{th}, of the total radio emission and their optical sizes as well as between f_{th} and the total 1.49 GHz radio luminosity (Figs. 2a and b). The one object not fitting these correlations is Mkn 527, which matches the definition of an H II galaxy only poorly; its H II region and the extent of its radio emission is relatively small and concentrated at its nucleus. An attempt to explain these correlations based on the diffusion lifetimes of CRE in the sample galaxies is the subject of a forthcoming publication.

The universality of the relation between f_{th} and galaxy sizes and luminosities can be put to test by studying a larger sample of galaxies for which reliable thermal-nonthermal separations and optical diameters are available. It might also be possible that this relation is restricted to H II galaxies; i.e. galaxies in which there are relatively large star forming regions. If this relation holds true, the isolation of the size or the absolute radio luminosity as a parameter in the strength of the non-thermal emission would allow a better estimate for the conversion between the SN rate and the observed non-thermal emission.

Another interpretation of the relative strengths between thermal and nonthermal emission is possible, using the steepenes of the radio spectral index. The radio emission is the sum of the thermal and nonthermal emission, and the spectral index of the thermal radio emission is *alpha* = -0.1, whereas the nonthermal radio emission is much steeper with *alpha* = -0.6 to -0.8. The spectral index of the total measured radio spectrum can therefore be used as a rough indicator for the relative strengths between thermal and nonthermal radio emission. Perez-Olea & Colina (1995) produced a series of model calculations of compact starbursts, giving the spectral index between the 6 and 20cm (1.49 and 5 Ghz) emission, $\alpha(6,20)$ as a time-dependent output parameter. Their models cover a variety of IMF slopes, and lower and upper cutoffs for the stellar masses, but their major division is one into models based on IB, or CSFR scenarios (see section 2.1). In general, in the IB models, $\alpha(6,20)$ is close to -0.1 for the first 4-6 Myrs after the burst, indicating radio spectra that are dominated by thermal emission. After 4-6 Myrs, with the onset of SN explosions, the nonthermal emission begins to dominate, and the spectral index increases rapidly to about -0.7. In the CSFR models, the spectral index is also close to -0.1 for the first 4-6 Myrs, but then decreases much slower to values of -0.4 to -0.6, as can be expected due to the continous generation of Lyc-emitting hot young stars. The values for $\alpha(6,20)$ of our sample galaxies vary between -0.27 and -0.75, with considerable error bars (see Table 1). The value of $\alpha(6,20) = 0.27$ for II Zw 40 indicates a young, thermally dominated starburst, that could be explained that Perez-Olea & Colina models do not take into account effects onto the spectral index resulting from CR confinement, which may underly the dependence between f_{th} and size mentioned earlier by an IB or CSFR model. Only the value of $\alpha(6,20) = -0.75$ for Mkn 297 seems to clearly indicate a nonthermally dominated radio spectrum, that has to result from an older starburst with relatively few Lyc-emitting hot stars still left. The values for $\alpha(6,20)$ as well as for $f_{th,1.49}$ of the other galaxies are such, that they agree best with CSFR models and bursts that are more then about 5 Myrs old. We note however, that the efficiency of the non-thermal radio emission from SNe is still rather poorly known - it certainly depends on the strength of the magnetic field -, and nonthermal emission may scale non-linearly with the number of SNe. Also, Perez-Olea & Colina's models do not take into account the effects onto the spectral index resulting from CR confinement, which may underly the dependence between f_{th} and size mentioned earlier.

2.3. Long term SFRs from B band luminosities

The B band luminosity can in principle be used to derive the SFR averaged over a time of about 1 Gyr, provided that the SFR did not change markedly in time (i.e. continous SF is assumed). The time scale which is indicated by the B band luminosity is very uncertain, causing SFRs based on the blue luminosity to vary widely between authors. Also, blue luminosities have been quoted in the literature in inconsistent ways as well. This confusion seems to appear mostly from the use of different definitions of the blue luminosity in term of solar luminosities, $L_B/L_\odot$, as has been noted by Thronson and Telesco (1986). Some authors, e.g. Thuan and Martin (1981) quote L_B in units of the solar luminosity seen through the B-passband.

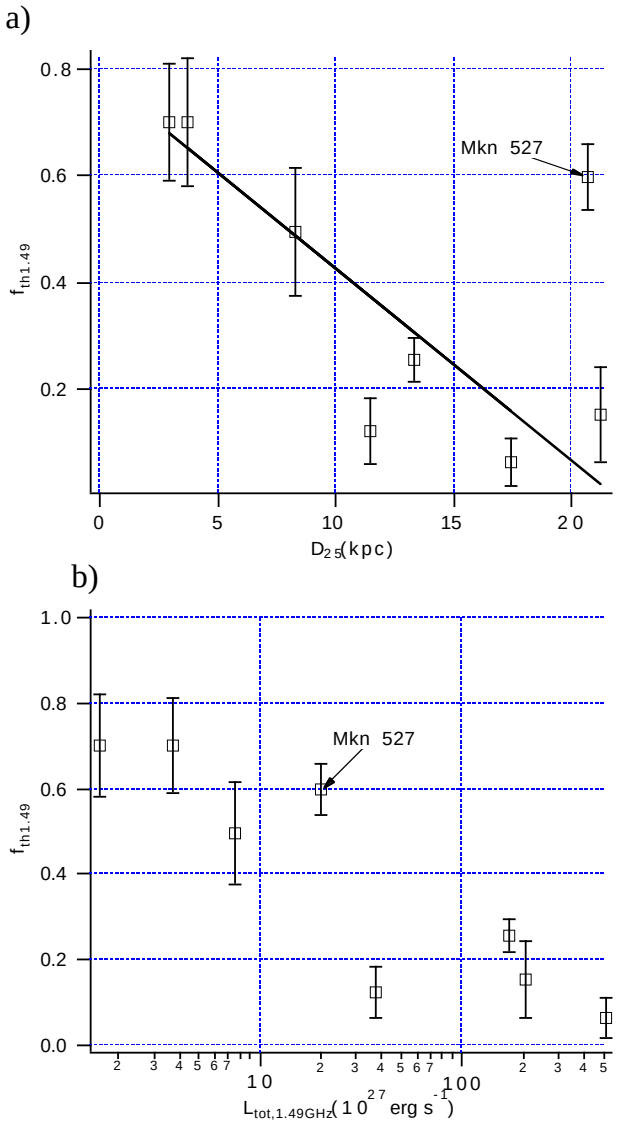

Fig. 2. a) The thermal fraction f_{th} at 1.49 GHz versus the optical diameter of the sample galaxies. The solid line is a least squares fit to the data, disregarding Mkn 527, resulting in: f_{th} = 0.784 - 0.0358 D_{25}(kpc). b) The thermal fraction f_{th} at 1.49 GHz versus the total radio luminosity at 1.49 GHz.

With $M_{B,\odot}$ = 5.48 (Allen, 1973; §75) they use f(L_B,L $\odot$) = $155.6 \cdot 10^{(-M_{B,\odot}/2.5)}$. Gallagher et al. (1984), Thronson and Telesco, as well as Sage et al. (1992) use for L_B = 1L$\odot$ the sun's bolometric luminosity of $3.8 \cdot 10^{33}$ erg s^{-1}. Based on the flux through the B-band of $6.475 \cdot 10^{-6}$ erg cm^{-2} s^{-1} from an object with m_B = 0.0 (Allen, §96), this leads to the conversion that is also used for this work:

$$\frac{L_B}{L_\odot} = 20.38 \cdot 10^{(-M_{B,\odot}/2.5)} \quad (9)$$

Eq. (9) gives values about 7.6 times smaller than used by Thuan and Martin. Thronson and Telesco as well as Sage et al. both derive formulae for the SFRs from Gallagher et al. (1984) who used a nonstandard notation for SFRs. Thronson and Telesco derive: SFR(M$\odot$ yr^{-1}) = 6.5 10^{-9} L_B(L$\odot$) which results in SFRs which are very large. Indeed, they conclude that in their sample of active star-forming dwarf galaxies, only a small fraction of galaxies do have current SFRs (based on FIR measurements) that are *higher* than the longer term SFRs based on B band luminosities. A re-derivation[3] of the SFR based on Gallagher et al. resulted in:

$$\frac{SFR_B}{M_\odot yr^{-1}} = 1.68 \cdot 10^{-10} \frac{L_B}{L\odot} \quad (10)$$

for $0.1M\odot \leq M \leq 100M\odot$ and assuming continous star formation. Using the Salpeter IMF again, the average SFR for stars with M > 5M$\odot$ is then given by:

$$\frac{SFR_B(M \leq 5M\odot)}{M\odot yr^{-1}} = 0.29 \cdot 10^{-10} \frac{L_B}{L\odot} \quad (11)$$

The SFRs calculated with eq. (11) are included in Table 2. The star formation rates based on B band luminosities are significantly lower than the current, or recent SFRs over the last few Myrs. However, this interpretation is correct only, if the galactic disk underlying the HII regions is over 1 Gyrs old, since this is the 'averaging timescale' assumed in eqs. 10 and 11. If the HII galaxies are genuinely young, then SFRs derived from B band luminosities will be sytematically too low, and SFRs derived by eqs. 10 and 11 should be multiplied by (1Gyr/age). We note that the SFRs derived from the B band are low enough to be sustainable over time scales of a Hubble time, since a division of the H I masses of the sample galaxies (Thuan and Martin, 1981, Gordon and Gottesman 1981) by the SFR shows a sufficient supply of H I. In contrast, if the much higher current SFRs would be at a constant level, the H I would be depleted in a few 100 Myrs.

2.4. Star formation histories from optical colors?

The surface colors presented in Paper I can be used to derive information about the composition of the stellar populations of the galaxies. Their B-R colors are an indicator of 'recent' (within time scales of 10^9 years) star forming activity, are bluer than typical disk colors which are assumed to be between 0.95 to 1.6. More recent star forming activity - within the last $3{\cdot}10^8$ years - is indicated by U-B colors which should be bluer than the typical range

[3] The SFR is commonly defined as the mass of stars born per year in a certain mass intervall. Gallagher et al. (1984) however give the SFR as indexes '*alpha*' which describe the *number* of stars born per year per mass intervall (see their eq. 1). To convert Gallager et al.'s SFR (their eq. 7): $\alpha_L \approx 0.29 \cdot 10^{-10}(L_B/L\odot)$ for a mass interval of 0.1 to 100 $M\odot$ into the common usage of SFR, a factor of 5.8 (as noted by Gallagher et al. in the paragraph below their eq. 1) needs to be applied to, resulting in eq. 10 of this text. This factor has been ommited by Sage et al. (1992), and they obtain extremely low SFRs from B band measurements.

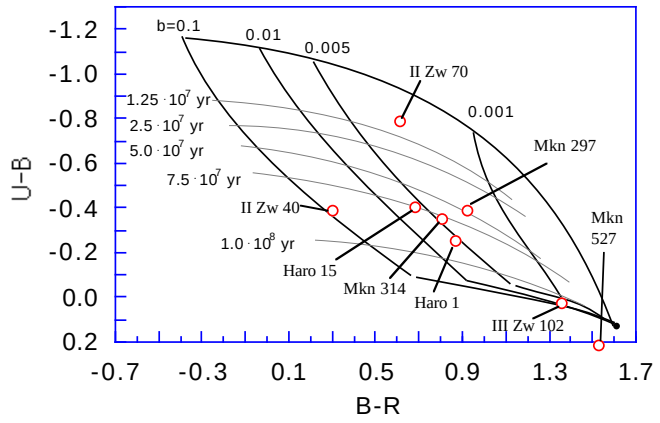

Fig. 3. Evolutionary tracks from stellar synthesis models with a low mass cut-off in the IMF of 5 M⊙ , taken from Krüger et al. (199 1), with the sample galaxies included. The solid lines indicate a constant burst strength, b, the dashed lines indicate the age since the star burst.

of -0.15 to 0.15. Unfortunately, no measurements of U colors could be taken and values from the literature (Thuan and Martin,1981; de Vaucouleurs et al. 1991) were used.

The approach taken in this section is to compare the measured galaxy colors with results from stellar synthesis models for galaxies from the literature. Stellar synthesis has been performed mostly for the optical/near IR wavelengths, e.g. Bruzual and Charlot (1993), Charlot and Bruzual (1991), Bruzual and Charlot (1993), Olofsson (1989), Krüger. et al. (1991) but also at UV wavelengths (Lequeux, 1981; Fanelli et al., 1988). The often cited papers by Thuan (1983) and Kennicutt (1983) are based on burst models by Larson and Tinsley (1978), Larson, Tinsley and Caldwell (1980), and Struck-Marcell and Tinsley (1978). Models considering radio and FIR emission are developed in the aforementioned papers, MK91 and M92. For an analysis of the colors of the H II galaxies discussed in this work, we use the predictions from the stellar synthesis models by Krüger et al. (1991), which were specifically created for star forming and metal poor dwarf galaxies. Their models allow estimates of the burst strengths and the time since the burst. The length of the burst itself , i.e. the time of an enhanced SFR, is relatively short and assumed to be $5 \cdot 10^6$ years. The models depend mostly on the low mass cut-off in a starburst. Scalo (1987) indicates that only stars more massive than ~ 4 M⊙ are formed in starbursts. The other, but not so crucial parameter, is the history of the star formation of the underlying disk, which is assumed to be exponentially decaying with a time scale of 10^9 years since the galaxy's formation; the starburst is occuring 15 Gyrs after the galaxies' formation. Earlier bursts are not excluded, but their influence on the colors of the current starburst is insignificant. Fig. 3 shows the evolutionary tracks in the U-B versus B-R color plane for a lower mass cutoff $m_{lb} = 5.0$ M⊙ taken from Krüger et al. The solid lines are loci of constant burst strength b, defined by

$$b = \frac{\text{total mass of stars formed during the burst}}{\text{total mass of stars ever formed in the underlying galaxy}}$$

and the dashed lines are of constant time since the starburst. The burst strength is strongly dependent on the assumed value for m_{lb}, whereas the age of the burst varies relatively little. The results of applying that model to the colors of the HII galaxies are given in Table 4. For the U-B colors in Table 4, colors measured within the effective aperture of the galaxies are taken if available (from Table 3b of Paper I), and integrated colors over the entire galaxy otherwise. B-R colors, are within apertures corresponding to the apertures of the U-B colors and taken from Table 3a of Paper I. Using these B-R and the U-B values, the model gives the burst strength b and the time since the burst, T_b. No results from the evolutionary synthesis models can be given for Mkn 527, as its integrated colors do not indicate the presence of any recent starburst.

3. Discussion

In the preceding sections we derived two sets of indicators: Star Formation *Rates* (see Table 1) and indicators for the *age* since a major change in the star formation rate occured. These age indicators are (Table 5): $T_{FIR,IB}$ based on the ratio of FIR/thermal radio emission (Section 2.1) and T_b on the B-R surface colors of the galaxies (Section 2.4). Further indicators for the age have been derived from the analysis of the radio spectra by DBDKS (with an update in Paper I). In these papers, models describing the history of the Cosmic Ray Electron (CRE) injection into the ISM have been fitted to the radio spectra with knees, which are present in three sample galaxies. The CRE injection is thought to result from SN explosions, and hence from stars which have formed at least 3 Myrs *earlier*. The radio frequency at which the knee in the spectrum occurs, the magnetic field strength in the galaxy, and the type of CRE injection model used determines the 'synchrotron age' T_{sync}, which is the time since a major change in the injection of CRE occured. Two types of models were fitted: One which describes a 'turn-on' of Cosmic Ray injection at a time $T_{sync,on}$ ago (from the onset of a number of SN explosions at about the same time), and another model, which describes either a one-time injection or a turn-off of the CRE injection (the spectral shapes and the times derived are identical in these cases). Discrimination between these two subcases may be possible by a consideration of the relation between the observed spectral index and the steepness of the CRE injection spectrum (Deeg, 1993). The turn-on model gave good fits to Mkn 297 and III Zw 102, and a mediocre one for Haro 15. For Haro 15, a one-time CRE injection 6 Myrs ago is likelier which is also a possibility for Mkn 297 and II Zw 102, but results in injection times which are very recent. The same goes

Table 4. Ages and strengths of the starbursts from stellar colors

Name	Haro 15	II Zw 40	Haro 1	II Zw 70	Mkn 297	Mkn 314	Mkn 527	III Zw 102
U-B	-0.40	-0.39	-0.25	-0.79	-0.39	-0.35	0.22	0.03
B-R	0.68	0.30	0.87	0.61	0.92	0.81	1.53	1.36
b	0.008	0.02	0.005	0.003	0.002	0.004	...	¡0.001
T_b(Myrs)	75	80	80	10	40	70	...	100

Table 5. Ages of the star burst in Myrs from several indicators

Name	Haro 15	II Zw 40	Haro 1	II Zw 70	Mkn 297	Mkn 314	Mkn 527	III Zw 102
T_b	75	80	80	10	40	70	...	100
$T_{syn,on}$	(13)	...	...	...	7	...	...	10
$T_{syn,off}$	...	...	...	...	(0.6)	...	...	...
$T_{syn,1time}$	6	...	...	...	(0.6)	...	...	(2.0)
$T_{FIR/th,IB}$	2.5	0	6	0	9	3	9	9

Notes to Table:
T_b : from Table 4, time since burst of 5 Myrs duration has ended, b ased on stellar colors.
$T_{syn,on}$: time since cosmic ray electrons (CRE) began to be inject ed into ISM. This value is similar to t' and fit model I_2 in Table 6 of DBDKS. Additional radio flux measurements and a re-evaluation of the CRE's inverse Compton loss rate (Paper I) led to values several times larger for Haro 15, whereas for Mkn 297 and III Zw 102 the changes are minor. Fits with poor significance are in brackets.
$T_{syn,1time}$: time since a one-time injection of CRE into the ISM o ccured. This value is similar to t' and fit model I_1 in Table 6 of DBDKS. The same comments as for $T_{syn,off}$ apply.
$T_{syn,off}$: time since CRE ceased to be injected into ISM. This va lue is similar to $T_{syn,1time}$.
$T_{FIR/th,IB}$: from Table 3, time since an instantaneous (delta shap ed) starburst occured, using M92's simulations

for the possibility of a CRE injection turn-off in Mkn 297 only 0.6 Myrs ago. Below, we first discuss results from the age indicators, and then the SFR indicators.

3.1. Comparison of the age estimates

The times T_b from derived stellar colors are larger by two orders of magnitudes than the ages $T_{syn,on}$ from synchrotron aging for the scenario of a sudden turn-on of CRE injection. T_b is also larger by one order of magnitude than the ages estimated from the ratio of FIR and thermal luminosities of Section 2.1. Considering the large uncertainties of the FIR to thermal radio ratio, the synchrotron ages T_{syn} and $T_{FIR/th}$ appear in agreement with each other. What then causes the large discrepancies between synchrotron ages and the burst ages from optical colors, and is that discrepancy real? A first answer might be, that the synchrotron ages, are not correct, and the color photometry gives the 'real' answer. However, besides the synchrotron ages, there is ample evidence for current or at least, very recent star forming activity. This is the presence of H II regions, with their FIR and thermal radio emission, all indicating a relatively high current or very recent (order of Myrs) SFR, and nonthermal radio emission, indicating significant numbers of supernovae over the last few Myrs. So, it is safe to conclude (with the possible exception of Mkn 527) that all of these galaxies have star forming activity which is much more recent than indicated by the optical colors. But what would then cause the starburst to be so misrepresented, or hidden, by optical colors?

Due to the absence of surface U-B color maps (only integrated U-B colors are available) it is only possible to position the galaxies in the color-color diagrams (Fig. 3) based on their integrated disk colors. The indicators of current star formation, such as Hα and radio emission, all originate in the localized star forming regions. Once resolved U-band photometry of the star forming regions is available, it will be possible to position just these regions on the color-color diagrams, and much shorter burst ages are expected, perhaps on the order of the age $T_{FIR/th}$. An additional uncertainty is added to the stellar colors by the absence of any good estimate for the galaxies' internal color excess, which can not be obtained due to their irregular morphology and localized dust content. As the color excess manifests itself in a reddening of the stellar colors, the true stellar colors may be significantly bluer, leading to much shorter times T_b.

Another major factor which probably limits the usefulness of stellar colors to derive burst ages is that the time-domain and time resolution observed through color-color diagrams is on a coarser time scale (10^{7-8} yrs) than synchrotron aging scales (10^6 yrs) and the scales of a few Myrs of the 'current' star forming rates from thermal radio or FIR emission. It is therefore quite possible that the stellar colors record the current *and* previous events which occured on the order of 10^{7-8}yrs ago.

3.2. Conclusions from the star formation indicators

Based on the star formation indicators which have been discussed in this chapter, an attempt is made to describe the state of the galaxies' star formation, sorting them in increasing age of their star formation event. A star formation event is assumed to last for 5 Myrs with approximately constant SFRs; no 'synchrotron aging' is detectable throughout this period. After that time, aging might be seen, telling us how far we are past the most active phase. The radio spectra will not indicate ages older than a few Myrs, beyond which the FIR-to-thermal ratio indicates time scales of 10^7 years. For longer term SFRs averaged over the last Gyr, the B band luminosities are taken.

II Zw 40 and II Zw 70 have relatively large but compact H II regions of roughly circular shape. Their thermal emission is relatively strong. II Zw 40 may be a very young, ongoing starburst, in which only a few SNs have occured to date. II Zw 70 has significant nonthermal emission, but strong thermal emission as well. The presence of strong thermal emission poses somewhat of a problem, as the nonthermal emission in II Zw 70 has a very steep spectral index. If it is emitted by young CRE (unsteepened by synchrotron or Inverse Compton losses, see DBDKS), this would indicate an extremely steep spectral index of the injected CRE of $\gamma_o = 3.4$. The other possibility is, that a steepened CRE spectrum from an older CRE injection with $\gamma_o = 2.4$ is observed (The values for $\gamma_o$in Table 6c of DBDKS are based on that assumption). Similarly to the calculations by DBDKS, who derive a synchrotron age T_{syn} for galaxies with knees in their spectra, the absence of such a knee in the observed frequency range indicates a time span in which the CRE injection did *not* change significantly (Deeg, 1993). In the case of II Zw 70, a spectrum consisting of steepened CRE would require an age of the CRE of $\gtrsim 30$ Myrs, which appears inconsistent with the presence of strong thermal emission that indicates star formation throughout the last 3 Myrs. It is therefore likely that II Zw 70 has a young starburst, possibly in addition to an older ($\gtrsim 30$ Myrs) one. The presence of a young starburst in II Zw 70 is also supported by Weiland (1991), based on results from a radio-optical evolutionary synthesis model. In contrast, Weiland cannot derive consistent optical and radio luminosities for II Zw 40, and attributes this to a relatively large influence of an underlying older stellar population, although the inconsistency may also be caused by the unreliability of the integrated photometry of that galaxy due to its highly irregular shape.

Basically the same discussion applies to Mkn 314 and Haro 1, only that the thermal emission is relatively lower. As in II Zw 70, Mkn 314's synchrotron spectrum is probably not steepened yet, and the CRE's age is less than ≈ 9 Myrs, indicating ongoing or very recent (a few Myrs ago) star forming activity. In Haro 1 we probably observe a steepened synchrotron spectrum, but in this case this would only mean that the CRE's age is $\gtrsim 0.6$ Myrs. An unsteepened synchrotron spectrum would indicate synchrotron ages of $\lesssim 0.3$ Myrs which seems to be too short.

III Zw 102 and Haro 15's spectra are dominated by nonthermal emission presumably from SNe, indicating star formation significantly older than ≈ 3 Mys. For Haro 15, the good fit for the one-time CRE injection scenario indicates that the star formation may have peaked several Myrs ago. III Zw 102 is very dust rich. Besides affecting the stellar colors (which are intrinsically bluer) the dust component may cause an excess in the FIR emission. This view is also supported by a comparison of the SFRs from Table 2, where the SFR based on FIR is by far the highest. Application of the measured FIR/L_{th} is only compatible with a model of an instantaneous burst, occuring at a time of $T_{FIR/th,IB} \approx 9$ Myrs ago (see Fig. 1 and Table 3). The only interpretation that agrees with the radio spectra, however, is a somewhat older star formation that has been *ongoing* since about 10^7 yrs, and that III Zw 102 has an FIR excess, indeed.

Mkn 297 consists of a large number of H II regions (Fig. 5 in DBDKS) and we probably observe a mixture of star formation of several ages in the various H II knots. This galaxy has the relatively lowest thermal radio emission (see f_{th} in Table 1) indicating that the current star formation has fallen below the level of a few Myrs ago in a majority of the H II knots. The age $T_{FIR/th}$ is relatively high. It is very likely that, e.g., the nonthermal emission originates in different H II regions then the majority of the FIR emission, and an age classification is difficult. In Mkn 297, we might observe a mix of the stages which are prevalent in the other galaxies.

All of the target galaxies show star formation rates which have been enhanced for at least the last few Myrs over the long term ($\approx$ 1Gyr) average given by the B-Band luminosity. We do not find indications for previous starbursts, or support for the view that H II galaxies are genuinely young objects, as has been suggested based on their generally low metallicities. The galaxies in the sample do have an underlying, older population. As is noted in paper I, all galaxies -except Mkn 527- have been suggested in the literature to be part of a merger or an interacting system, which might trigger the star formation and its associated radiation.

3.3. Outlook

The work described in DBDKS, paper I and here has compared and derived star formation rates from a variety of different methods. Those using the radio-continuum emission have been applied for the first time to a sample of galaxies in a homogeneous way and have been compared to determinations of the star formation history from other wavelength domains. A combined analysis of radio continuum spectra, Ha, FIR, and eventually UV data can result

in a consistent description of the current and very recent star formation rate, as well as give age indicators for recent star formation events. For these very recent star formation events occuring in H II galaxies, optical data appear to lack the time resolution and are also much more prone to uncertainties from extinction.

The approach outlined in these papers can certainly be verified and extended by investigations of different samples of galaxies. Spectral turnovers, although generally being smoother (with a change of spectral indices of $\delta\alpha \approx 0.5$) and spread out over a larger range of frequencies, have been observed in normal spiral galaxies by several authors (e.g. Israel and Mahoney, 1990, Israel, Mahoney and Howarth, 1992; Pohl, Schlickeiser and Hummel, 1991; Pohl, Schlickeiser and Lesch, 1991) who reached different, and sometimes conflicting conclusions. For example, Israel and de Bruyn (1988) attribute the cause of the spectral breaks to free-free absorption at low frequencies. Free-free absorption depends on the existence of a cool ionized medium of a few 100k. For the same sample, Hummel (1991) favors a model of CRE propagation losses causing spectral breaks - a model which has been discounted by DBDKS for this H II galaxy sample. In the spirals investigated by these authors, generally some star formation does take place, but it is not as dominating an event as in the case of H II galaxies, and the star formation can be expected to take place over longer periods in time. A comparative study of these normal spirals, analyzing optical and FIR data as done in this work, may show if the spectral turn-overs in spirals are caused by the same star-formation-related mechanism as in HII galaxies, or by different ones based on the galaxy geometry, such as galactic wind models as proposed by Pohl et al.

An other alternative would be the study of nearby dwarf galaxies such as the Magellanic Clouds or Holmberg II (Puche et al. 1992), in which significant star formation is seen. In these studies, the investigation of star formation rates and histories for single star forming regions should be possible. In the case of the Magellanic Clouds, data at various bands are readily available (for references, see Westerlund, 1990; for individual clusters see his Table 7). The integrated radio spectra of the LMC and the SMC both have significant thermal emission and do not show spectral breaks (Haynes et al. 1991) down to frequencies as low as 100 MHz. This does not exclude, however, the presence of spectral breaks in local star forming regions. The radio data have been compared only to FIR results (Xu et al., 1992), and comparative studies between the radio emission and Hα (Kennicutt and Hodge 1986) or stellar colors (e.g. Garmany et al. 1987) should allow a thorough study of the local star formation processes and histories.

The relation between the CRE injection rates and the nonthermal spectra has been investigated so far only for a few models in which CRE injection rates were instantaneously turned on or off. These models could be refined to create model synchrotron spectra for arbitrary variations of the CRE injection rate, building the radio spectra from a series delta shaped CRE injection events. This would allow the construction of synchrotron spectra which could realistically account for the amount of CRE injected into the ISM, during and after a star burst. The injection rate is given by the rate of stars which become supernovae. To some degree the mass of the SN progenitor star might play a role in the amount of CRE produced per SN as well. The rate of SNe over time after a starburst depends mostly on the assumption used for the IMF, and might decrease or stay relatively constant, until the stars with lowest possible mass have turned into supernovae.

The results of the current sample are intended to be tied in with a study of their H I emission. For half of the sample galaxies H I maps already exist, most of which show sings of mergers or interactions. Taylor et al.'s (1993) H I map of Mkn 314 shows the presence of small companion galaxies, and Brinks and Klein (1988) identified II Zw 40 with an H I cloud that has a nearby counterpart of about equal mass, but is invisible at optical wavelengths. The strong radio emission was the main selection criterion for our sample from the much larger pool of starforming H II galaxies. Could it be that only a merger/interaction develops a starburst which gives rise to a strong radio continuum emission? Could these galaxies be scaled down versions of superluminous IRAS galaxies, all of which are thought to be remnants of mergers (e.g. Kormendy and Sanders, 1992)? Does the HI show signs of interaction that are not evident or ambiguous from optical data? Is there evidence for ordered motion in the more luminous systems, and is the H I largely confined to the disk, or are there discrete blobs of HI? Lo, Sargent and Young (1993) observed faint dwarf galaxies and found a clumpy H I medium with chaotic velocities, that is not gravitationally stable for longer than 10^8yrs, leading to the speculation, that some faint dwarfs were starforming galaxies earlier in their life. If the H I observations of our sample should show large ordered motions, this might imply the existence of two classes of H II galaxies: Radio-loud ones with strong star formation triggered by a merger or interaction (the strong radio emission was a selection criterion for inclusion into this study!), and radio-quiet ones, with a more chaotic H I distribution and less intense, stochastic star formation. The latter category would then correspond to faint dwarfs undergoing a burst of star formation. These are the questions we would like to address in the future.

4. Summary

A sample of actively star forming H II galaxies, distinguished by relatively strong radio continuum emission, has been observed in the radio continuum, in optical broadband colors, as well as in narrow band Ha. These galaxies are currently undergoing very active star formation, indicated by the presence of one or more giant H II regions.

They are of varied underlying morphologies, with irregular or amorphous galaxies dominating the sample.

Radio continuum observations at 0.32, 1.5, 8.4 and 15 GHz were obtained at the VLA. Supplemented by flux density measurements taken from the literature, radio spectra for the target galaxies were constructed in the range from 0.32 to 15 GHz. The spectra of several of the galaxies (Haro 15, Mkn 297, III Zw 102) were found to flatten towards lower frequencies, which is unusual. The spectra of two galaxies (Mkn 527 and II Zw 70) are conventional, concave spectra. One galaxy (II Zw 40) is dominated by thermal emission throughout its spectrum, which is also unusual for a galaxy spectrum. The spectra of two galaxies (Mkn 314, Haro 1) cannot be classified well, due to a lack of frequency coverage or too large uncertainties in the flux measurements. Because integrated B and R band photometry as well as quantitative Hα observations had been published for only a few galaxies, all galaxies were observed by us in the B, R, and I band and in the Ha emission line. Homogeneous surface and aperture photometry was obtained for the entire sample in all of the aforementioned bands. An overview of the literature concerning each target galaxy and its morphology is given in Paper I and in DBDKS. Classification of the galaxies in the Hubble system are uncertain and sometimes contradictory. It was found that all, except one of the sample galaxies -Mkn 527-, have been described by at least one author to be a merging or interacting system. The H II galaxies described in this work were chosen to be those with the highest radio continuum emission, so this might be a selection effect. The radio spectra, Ha photometry, as well as UV observations from the literature were used to derive the fraction of thermal emission in the galaxies. This could be done with a higher reliability than what is usually achieved on the basis of just one set of data. A correlation between the fraction of thermal emission and the size, as well as the total luminosity, of the galaxies has been found, the meaning of which is not immediately obvious.

Using a variety of indicators, star formation rates of the galaxies have been derived. Thermal radio emission, non-thermal radio emission, and FIR emission all indicate enhanced star formation through the last 10^{6-7} years. For all galaxies, these recent star formation rates are higher than the long term ($\approx$ 1 Gyr) rates based on B band data. Also employed were measures for the *age* of the star formation events, such as synchrotron aging which is based on the radio spectra, the thermal-radio to FIR ratio, and optical colors. The measures based on radio or Hα emission indicate changes in the starforming activity in the last few Myrs in agreement with the finding of enhanced star formation rates. Additionally, from the radio spectra one can derive details about the recent star formation history (i.e. if there was a turn-on or turn-off in star formation, or if there have been periods of quiescence). In some galaxies with knees in their spectra (e.g. III Zw 102 and Haro15), a peak in the SF activity a few Myrs ago is indicated. In others (e.g. IIZw 70, Mkn 314), which show no knees, the steepness of the spectra can be used to limit the age of the star forming event. Age indications based on optical colors are restricted to indicate star forming activity on scales of larger than 10^{7-8} yrs and are affected by extinction in the sample galaxies. They are therefore not very useful to probe SF histories on timescales of 10^{6-7}yrs, as is the case in H II galaxies. Based on the information gained about the star formation rates and ages, the galaxies were sorted into a sequence of the age of their starbursts. From this combination of star formation rate and age indicators, support is found that both the thermal and non-thermal part of the radio emission are valid indicators for star forming activity and that radio spectra can be used to determine the age of a recent star forming event that is not older than 10^{6-7} yrs.

A major result of this work is the demonstration that we have a good understanding of the physical picture of a region of active star formation, with subsequent SNe going off, which give rise to a mix of thermal and nonthermal radio continuum emission. Moreover, it has been shown that the detailed shape of a radio continuum spectra can be used to set limits on the age of recent bursts of star formation. The time resolution is of the same order as that obtained from Hα imaging and is much higher than can be obtained from broad band (optical) colors. As such, radio continuum imaging, combined with Hα photometry, is a valuable tool in determining star formation rates and histories, not only in H II galaxies, but in galaxies in general.

References

Allen 1973, Astrophysical Quantities, Third Edition (London : Athlone Press)
Belfort, P., Mochkovitch, R., Dennefeld, M.,1987 A&A, 176, 1
Brinks, E., Klein, U. 1988, MNRAS, 231, 63p
Bruzual, G.A., Charlot, S. 1993, ApJ, 405, 538, Spectral evolution of stellar populations using isochrone synthesis
Charlot, S., Bruzual, G. 1991, ApJ, 367, 126
Condon, J.J. 1992, ARA&A 30, 575
Condon, J.J., Yin, Q.F. 1990, ApJ, 357, 97
Deeg, H.J. 1993, PhD. Thesis, The University of New Mexico
Deeg, H.J., Duric, N., Brinks, E. 1997, A&A, 323, 323 (Paper I)
Deeg, H.J., Brinks, E., Duric, N., Klein, U., Skillman, E. 1993, ApJ, 410, 626 (DBDKS)
de Vaucouleurs, G., de Vaucouleurs, A., Corwin, H.G., Buta, R.J., Paturel, G., Fouqué, P. 1991, Third reference catalog of bright galaxies (RC3) (New York: Springer Verlag)
Fanelli, M.N., O'Connell, R.W., Thuan, T.X. 1988, ApJ, 334, 665
Gallagher, III, J.S., Hunter, D.A., Tutukov, A.V. 1984, ApJ, 284, 544
Garmany, C.D., Conti, P.S., Massey, P. 1987, AJ, 93, 1070

Gordon, D., Gottesman, S.T. 1981, AJ, 86, 161
Haynes, R.F., Klein, U., Wayte, S.R. et al. 1991, A&A, 252, 475
Hummel, E. 1991, A&A, 251, 442
Israel, F.P., de Bruyn, A.G. 1988, A&A, 198, 109
Israel, F.P., Mahoney, M.J. 1990, ApJ, 352, 30
Israel, F.P., Mahoney, M.J., Howarth, N. 1992, A&A , 261, 47
Kennicutt, R. 1983, ApJ, 272, 54
Kennicutt, R, Hodge P.W. 1986, ApJ, 306, 130
Klein, U., Weiland, H., Brinks, E. 1991, A&A, 246, 323
Klein, U., Wielebinski, R., Haynes, R.F. Malin, D.F., 1989, A&A, 211, 280
Kormendy, J., Sanders, D.B. 1992, ApJ, 390, L53
Krger, H., Fritze-von Alvensleben, U., Loose, H.-H., Fricke, K.J. 1991, A&A, 242, 343
Larson, R.B., Tinsley, B.M. 1978, ApJ, 219, 46
Larson, R.B., Tinsley, B.M, Caldwell, C.N. 1980, ApJ, 237, 692
Lequeux, J. 1980, in Star Formation (Saas-Fee: Geneva Obs), p. 75
Lequeux, J. Maucherat-Joubert, M., Deharveng, J.M., Kunth, D., 1981, A&A, 103, 305
Lo, K.Y, Sargent, W.L.W., Young, K. 1993, AJ, 106, 507
Mas-Hesse, J.M. 1992, A&A, 253, 49 (M92)
Mas-Hesse, J.M., Kunth, D. 1991, A&AS, 88, 399 (MK91)
Olofsson, K. 1989, A&AS, 80, 317
Perez-Olea, D.E., Colina, L., 1995, MNRAS, 277, 857
Pohl, M., Schlickeiser, R. 1990, A&A, 234, 147
Pohl, M., Schlickeiser, R., Hummel, E. 1991, A&A, 250, 302
Pohl, M., Schlickeiser, R., Lesch, H. 1991, A&A, 252, 493
Puche, D., Westpfahl, D., Brinks, E., Roy, J.-R. 1992, AJ, 103, 1841
Sage, L.J., Salzer, J.J., Loose, H.-H., Henkel, C. 1992, A&A, 265, 19
Sauvage, M., Thuan, T.X. 1992, ApJ, 396, L69
Scalo, M. 1987, in: Starbursts and galaxy Evolution, eds. T.X. Thuan et al. (Edition Frontières: Paris), p.445
Scoville, N.Z., Sargent, A.I., Sanders, D.B., Soifer, B.T. 1991, ApJ, 366, L5
Struck-Marcell, C., Tinsley, B.M. 1978, ApJ, 221, 562
Taylor, C.L., Brinks, E., Skillman, E.D. 1993, AJ, 105, 128
Thronson, H.A., Telesco, C.M. 1986, ApJ, 311, 98
Thuan, T.X. 1983, ApJ, 268, 667
Thuan, T.X., Martin , G.E. 1981, ApJ, 247, 823
Wilson, C.D., Scoville, N. 1992, ApJ, 385, 512
Wright, G.S., Joseph, R.D., Robertson, N.A., James, P.A., Meikle, W.P.S. 1988, MNRAS, 233, 1
Wunderlich, E., Klein, U., Wielebinski, R. 1987, A&AS, 69, 487
Xu, C., Klein, U., Meinert, D., Wielebinski, R. Haynes, R.F. 1992, A&A, 257, 47